

Fully transferable interatomic potentials for large-scale computer simulations of simple metal oxides: Application to MgO

Andrés Aguado*

Departamento de Física Teórica, Universidad de Valladolid, Valladolid 47011, Spain

Paul A. Madden

Physical and Theoretical Chemistry Laboratory, University of Oxford, South Parks Road, Oxford OX1 3QZ, United Kingdom

(Received 24 August 2004; published 2 December 2004)

Large scale computer simulations (those involving explicit consideration of a large number of atoms and/or very long simulation times) are needed in order to get a proper understanding of many material properties (phase transitions, transport properties, etc.). Given the computational cost associated with *ab initio* electronic structure codes, computational materials science and geoscience would greatly benefit from the availability of transferable, parameterized interatomic potentials. In this work, and taking MgO as test material, we show that fully transferable potential models may indeed be generated, by combining a physically motivated analytical form for the potential with an *ab initio* force-matching procedure to obtain the potential parameters. The potential is based on an ionic model of interactions, and incorporates many-body effects, to reflect the high sensitivity of the charge distribution of the oxide anion (and related properties, such as ionic polarizabilities, etc.) to the coordination environment. It is shown to describe accurately the atomic interactions in arbitrary coordination environments, so long as interionic electron transfer may be neglected. Close agreement with *ab initio results* is demonstrated for MgO in the bulk to extreme pressure, at point and extended bulk defects, and at planar surfaces and the corners and edges of clusters.

DOI: 10.1103/PhysRevB.70.245103

PACS number(s): 63.20.-e, 34.20.Cf, 61.46.+w, 68.35.Bs

I. INTRODUCTION

To find transferable potential models for the description of atomic interactions in ionic materials is one of the holy grails of computational materials science. A transferable potential should provide an equally accurate description of interatomic forces in a variety of environments including perfect and defective crystal structures and liquid phases, but also in low-coordinated atomic sites, such as those encountered at surfaces and in clusters. Such a potential would allow the efficient and realistic simulation of large-scale phenomena (both in the space and time domains) which nowadays lie outside the range of applicability of *ab initio* methodologies.

Potential parameters may be obtained by fitting to interatomic forces and stress tensor components evaluated *ab initio* for a large number of different atomic configurations. The work by Laio *et al.*¹ shows this so-called force-matching procedure leads to a potential for bulk iron that mimics the *ab initio* interactions for pressure and temperature conditions close to those employed in the reference *ab initio* calculations. However, with the simple form of their potential model, transferability is lost and a separate potential is needed for each different thermodynamic state. In this paper we show that, at least for a simple metal oxide like MgO, it is possible to write down an analytical expression for the potential that incorporates many-body features and independently describes all relevant components of atomic interactions (as extracted from quantum-mechanical perturbation theory).² When that expression is combined with the force-matching approach, a potential emerges which describes both bulk phases (for the whole range of pressures and tempera-

tures relevant to geophysical applications), lattice defects, different surface terminations and clusters with high accuracy. The potential is wholly derived from first principles and the range of transferability is much greater than achieved in previous attempts;³⁻¹¹ application of the same techniques should lead to *predictive* potentials for less well-studied materials.

The paper is structured in the following way: In Sec. II we describe the potential model and some details of the fitting procedure. In Sec. III we present some test calculations in order to demonstrate that our potential is transferable to arbitrary atomic coordination environments (as long as electron itineracy is not relevant). Finally, in Sec. IV, we summarize the main conclusions.

II. THEORY

The potential is dubbed “GAIM” because it is a generalization of the aspherical ion model (AIM) previously reported.³ The AIM is based upon the interactions between closed-shell Mg^{2+} and O^{2-} ions, so that charge-charge, polarization, dispersion and short-range overlap repulsion are the relevant interactions.² Charge transfer is not allowed and the ions have formal charges. The many-body character of interactions in MgO is due to high sensitivity of the electronic structure of the oxide anion to its coordination and electrostatic environment¹²⁻¹⁴ (remember that O^{2-} is not bound as a free species, but stabilized in a crystal by the lattice potential).

The AIM incorporates variables (induced dipoles and quadrupoles, and changes in the anion size and shape) that

mimic this changing electronic structure. The optimal values of these additional electronic variables are those which minimize the total energy for each atomic configuration, and must be calculated (in our case, by using a conjugate gradient routine) in order to obtain the correct forces acting on the atoms at each step of a molecular dynamics (MD) run. An AIM potential for MgO, parameterised by *ab initio* force-matching on a restricted set of disordered condensed-phase configurations, achieved a respectable³⁻⁷ yet not perfect transferability. In particular, when applied to small clusters, or to bulk phases at the very high pressure and temperature conditions relevant to geophysics, so-called polarization catastrophes (divergences in the self-consistent multipoles) were observed. The GAIM potential has almost exactly the same functional form as the AIM potential,⁴ but generalizes it in allowing the ionic susceptibilities, which govern the induced multipoles and ion size changes, to themselves depend on the ionic coordination environment. To better appreciate the differences between AIM and GAIM potentials, we describe here both potentials in full detail, even though the AIM model has already been described in Ref. 4.

The charge-charge and dispersion components of the AIM potential are purely pairwise additive:

$$V^{q-q} = \sum_{i \leq j} \frac{q_i q_j}{r_{ij}}, \quad (1)$$

$$V^{\text{disp}} = - \sum_{i \leq j} [f_6^{ij}(r^{ij}) C_6^{ij}/r^{ij^6} + f_8^{ij}(r^{ij}) C_8^{ij}/r^{ij^8}], \quad (2)$$

where q_i is the (formal) charge on ion i , C_6^{ij} (C_8^{ij}) is the dipole-dipole (dipole-quadrupole) dispersion coefficient, and f_n^{ij} are Tang-Toennies dispersion damping functions,¹⁵ describing the short-range penetration correction to the asymptotic multipole expansion of dispersion² (see below).

The overlap repulsion component is given by

$$\begin{aligned} V^{\text{rep}} = & \sum_{i \in O, j \in Mg} [A^{-+} e^{-a^{-+} \rho^{ij}} + B^{-+} e^{-b^{-+} \rho^{ij}}] + \sum_{i, j \in O} A^{--} e^{-a^{--} r^{ij}} \\ & + \sum_{i, j \in Mg} A^{++} e^{-a^{++} r^{ij}} + \sum_{i \in O} [D^{-}(e^{\beta^{-} \delta^i} + e^{-\beta^{-} \delta^i}) \\ & + (e^{\zeta^{-2} |\nu^i|^2} - 1) + (e^{\eta^{-2} |\kappa^i|^2} - 1)], \end{aligned} \quad (3)$$

$$\rho^{ij} = r^{ij} - \delta^i - S_{\alpha}^{(1)} \nu_{\alpha}^j - S_{\alpha\beta}^{(2)} \kappa_{\alpha\beta}^j, \quad (4)$$

where summation of repeated indexes is implied. The first three summations represent cation-anion, anion-anion and cation-cation short-range repulsions, respectively. In the cation-anion term, δ^i is a variable which characterizes the deviation of the radius of oxide ion i from its default value (the default ion radii have been subsumed into the preexponential terms). $\{\nu_{\alpha}^j\}$ is a set of three variables, for each oxide ion, describing the Cartesian components of a dipolar distortion of the ion shape. The magnitude and orientation of this dipolar deformation will be determined by the instantaneous positions of neighboring ions and will, therefore, change at each timestep in an MD run. Similarly, $\{\kappa_{\alpha\beta}^j\}$ is a set of five independent variables describing the corresponding quadrupolar shape distortions [In Eq. (3), $|\kappa|^2 = \kappa_{xx}^2 + \kappa_{yy}^2 + \kappa_{zz}^2$

$+ 2(\kappa_{xy}^2 + \kappa_{xz}^2 + \kappa_{yz}^2)$ and $S_{\alpha}^{(1)} = r_{\alpha}^{ij}/r^{ij}$ and $S_{\alpha\beta}^{(2)} = 3r_{\alpha}^{ij}r_{\beta}^{ij}/r^{ij^2} - \delta_{\alpha\beta}$ are interaction tensors.] We have assumed throughout the present work that these shape deformations do not affect significantly the anion-anion and cation-cation repulsions, which have been represented by simple Born-Mayer exponentials as if the ions were effectively spherical in their interactions with other ions of the same type. This simplification, which may not apply to other materials, will be tested by our ability to obtain an acceptable fit to the *ab initio* forces. The last summations include the self energy terms, that is the energy cost of deforming the charge density of an oxide anion. β , ζ , and η are effective force constants determining how difficult it is for a particular ion to be deformed in a spherical, dipolar or quadrupolar way.

The polarization part of the potential includes both dipolar and quadrupolar contributions,¹⁶

$$\begin{aligned} V^{\text{pol}} = & \sum_{i, j} \left((q^i \mu_{\alpha}^j [1 - \Delta_{ij} g_D^i(r^{ij})] - q^j \mu_{\alpha}^i [1 - \Delta_{ij} g_D^j(r^{ij})]) T_{\alpha}^{(1)} \right. \\ & + \left(\frac{q^i \theta_{\alpha\beta}^j}{3} [1 - \Delta_{ij} g_Q^j(r^{ij})] + \frac{\theta_{\alpha\beta}^i q^j}{3} [1 - \Delta_{ij} g_Q^i(r^{ij})] \right. \\ & - \left. \mu_{\alpha}^i \mu_{\beta}^j \right) T_{\alpha\beta}^{(2)} + \left(\frac{\mu_{\alpha}^i \theta_{\beta\gamma}^j}{3} + \frac{\theta_{\alpha\beta}^i \mu_{\gamma}^j}{3} \right) T_{\alpha\beta\gamma}^{(3)} \\ & + \frac{\theta_{\alpha\beta}^i \theta_{\gamma\delta}^j}{9} T_{\alpha\beta\gamma\delta}^{(4)} + \sum_{i \in O} (k_1^i |\vec{\mu}^i|^2 + k_2^i \mu_{\alpha}^i \theta_{\alpha\beta}^i \mu_{\beta}^i + k_3^i \theta_{\alpha\beta}^i \theta_{\alpha\beta}^i \\ & + k_4^i |\vec{\mu}^i \cdot \vec{\mu}^i|^2), \end{aligned} \quad (5)$$

where $\Delta_{ij} = 1$ if i and j refer to different ion species and zero otherwise, $k_1^i = 1/2\alpha^i$, $k_2^i = -B^i/4\alpha^i C^i$, $k_3^i = 1/6C^i$, $k_4^i = (2\gamma^i C^i - 3B^{i^2})/48\alpha^{i^4} C^i$, α^i and C^i are the dipole and quadrupole polarizabilities, and B^i and γ^i the dipole-dipole-quadrupole and nonlinear dipole hyperpolarizabilities of ion i , respectively (γ^i was not considered in our previous works, so its inclusion here represents an extension of the model). $T_{\alpha\beta\gamma\delta} = \nabla_{\alpha} \nabla_{\beta} \nabla_{\gamma} \nabla_{\delta} \dots 1/r^{ij}$ are the multipole interaction tensors,² with the superindex indicating the order of the operator. The charge-dipole and charge-quadrupole cation-anion asymptotic terms are corrected for penetration effects at short-range by using Tang-Toennies damping functions,¹⁵ namely

$$g_D^j(r^{ij}) = c_D^j e^{-b_D r^{ij}} \sum_{k=0}^4 \frac{(b_D r^{ij})^k}{k!}, \quad (6)$$

$$g_Q^j(r^{ij}) = c_Q^j e^{-b_Q r^{ij}} \sum_{k=0}^6 \frac{(b_Q r^{ij})^k}{k!}, \quad (7)$$

with D and Q standing for dipolar and quadrupolar parts and $j = +$ and $-$ for cations and anions, respectively. Note that the b_D and b_Q parameters, which determine the distance at which the overlap of the charge densities begins to affect the induced multipoles, are the same for both anions and cations, while the c_D and c_Q parameters, measuring the strength of the ion response to this effect, depend on the identity of the ion. The short-range induction corrections are neglected in

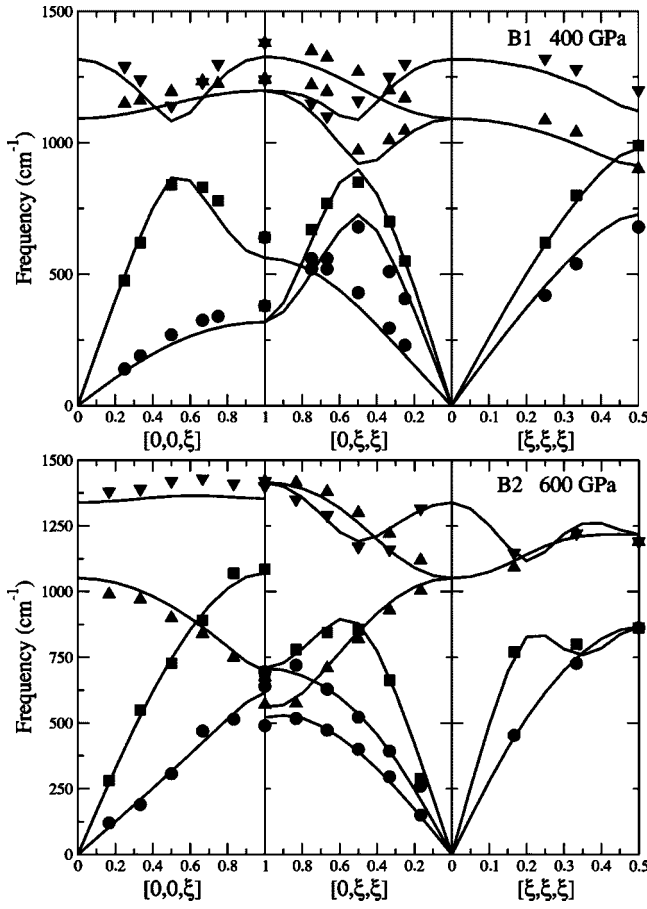


FIG. 1. Phonon dispersion curves for MgO at 300 K and several pressures, for both B1 and B2 crystalline phases. *Ab initio* results by Oganov *et al.* (Ref. 22) are shown as full lines. Symbols are the phonons predicted by the present model: Circles–TA mode; squares–LA mode; triangles–TO mode; inverted triangles–LO mode.

both anion-anion and cation-cation interactions. The same kind of damping function is used to screen the dispersion interactions at short distances (see above). In this case, the strength coefficients c are set to unity, so that only two range parameters, b_6^{ij} and b_8^{ij} (for dipole-dipole and dipole-quadrupole dispersion terms, respectively) are needed for each interacting pair.

We perform an Ewald summation of all electrostatic interactions⁷ and also of dispersion.¹⁷ Thus, all those interactions are free from truncation errors. The short-range repulsion, which is an exponentially decaying function of distance is, however, truncated beyond a distance equal to half the simulation cell length.

The ability of the charge density of ion i to polarize in response to electric fields and field gradients acting on it is controlled by its dipole (α_i) and quadrupole (C_i) polarizabilities, and dipole-dipole-quadrupole (B_i) and nonlinear dipole (γ') hyperpolarizabilities. The AIM model incorporates two other susceptibilities (η_i and κ_i) which control the ability of ion i to reduce the short-range overlap repulsion energy by undergoing shape distortions of dipolar and quadrupolar symmetry. All these parameters are constant in the original

AIM.³ This implies, for example, that polarization and overlap parts are decoupled: Induced multipoles can be obtained by minimization of the polarization energy, while size and shape distortions minimize the overlap energy component.

The main new ingredient in the GAIM potential is that the response properties themselves are allowed to be environmentally dependent (the functional form of the several potential components, described above, is exactly the same). Pyper has calculated *ab initio* values for the polarizabilities of oxide anions in different crystalline phases of MgO, and has noted¹³ that polarizability variations may be mostly explained in terms of changes in the size of the anion and in the strength of the stabilizing electrostatic potential field.

Following this line of thinking, we adopt the following simple expression for the dipole polarisability of ion i (assumed to be isotropic):

$$\alpha_i = \alpha_0 (e^{\alpha_\delta \delta_i} + e^{\alpha_V V_i^M}), \quad (8)$$

where δ_i [see Eq. (3)] is the variable describing the size of ion i and V_i^M is the Madelung potential at the position of ion i .⁷ α_0 , α_δ , and α_V are constants to be obtained from a force matching procedure. The signs of α_δ and α_V are such that anions of larger radii or under the action of a less intense Madelung potential have larger polarizabilities. Although it is clear that higher-order polarizabilities will change in the same manner,¹⁸ the effect has not been quantified, so we just assume that the ratios of each higher-order polarizability to α_i are constant:

$$B_i = B_0 \alpha_i \quad C_i = C_0 \alpha_i \quad \gamma_i = \gamma_0 \alpha_i, \quad (9)$$

where B_0 , C_0 , and γ_0 are again determined by force matching. The environmental dependencies of the shape deformation susceptibilities are analogous to those of the polarizabilities:¹⁹

$$\eta_i = \eta_0 e^{\eta_\delta \delta_i}, \quad \kappa_i = \kappa_0 \eta_i, \quad (10)$$

where η_0 , η_δ , and κ_0 are to be determined from force matching. Note that η_i and κ_i , which enter only the short-range overlap repulsion terms, do not depend explicitly on the Madelung potential. Within this formulation, the radii of the ions (δ_i) become the fundamental quantities, and polarization and overlap parts of the potential couple, so the optimal values of multipoles, size and shape deformations, and polarizabilities and deformation susceptibilities must be determined conjointly, by minimizing the sum of overlap and polarization energies.

In order to obtain optimal values for the many parameters entering the GAIM potential, the force matching procedure is applied to exactly the same set of *ab initio* calculations (performed using the density functional theory CASTEP code,²⁰ within the generalized gradient approximation²¹ to exchange and correlation effects) as in our previous works.^{3,4}

III. RESULTS

As a first test of transferability, we show in Fig. 1 phonon dispersion curves of both 6-coordinated rocksalt (B1) and 8-coordinated cesium chloride-like (B2) crystalline phases of

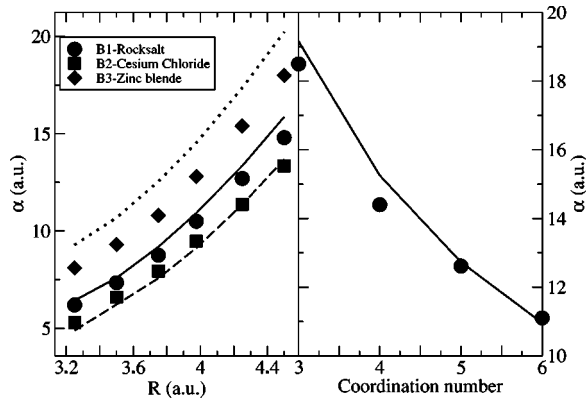


FIG. 2. Oxide anion polarizabilities for (left) three different MgO crystalline phases as a function of compression, compared to *ab initio* results (Ref. 13) and (right) symmetry inequivalent oxide anions in $(\text{MgO})_{64}$ cluster, as a function of coordination number, compared to *ab initio* results (Ref. 12). Symbols are potential model values.

MgO, at different pressures (we do not show corresponding results at zero pressure, because they are very close to those obtained with an AIM potential, already reported in Refs. 6 and 7). The agreement with the *ab initio* results by Oganov *et al.*²² is excellent, as the only difference is a slight and systematic overestimation of optic mode frequencies. The agreement is of a similar quality for all pressures between 0 and 600 GPa. Phonon dispersion curves represent a particularly stringent test for our model, as vibrational normal modes involve the participation of all electronic degrees of freedom, but to different degrees in different regions of the Brillouin zone (for example, at some particularly symmetric k -points, only quadrupoles are activated). The uniform agreement with the *ab initio* results demonstrates that the relative strengths of different terms in the potential are correct, as well as their variation with pressure and crystalline coordination environment. In particular, good reproduction of acoustic modes at low k implies that the variations of elastic constants with pressure are also properly reproduced. There is also good agreement in the longitudinal optic-transverse optic (LO-TO) splitting for all pressures. LO-TO splitting is a consequence of the coupling of long-wavelength longitudinal optic modes with macroscopic electric fields, themselves induced by the long-range nature of Coulombic interactions. The coupling constants are the Born effective charges,²³ which can be defined as the change in macroscopic polarization induced by a periodic displacement of all ions of a given species, along a particular direction, at zero macroscopic electric field. This change in polarization has an obvious ionic component and an electronic component, represented in this work by the ion polarizabilities. The correct pressure dependence of the LO-TO splitting thus implies that the pressure variation of the oxide polarizability has been properly captured. This is explicitly shown in Fig. 2, where model polarizabilities are compared to *ab initio* values derived by Pyper on the basis of coupled cluster calculations.¹³ The agreement is only semiquantitative in this case, most probably because our potential has been fitted to DFT results, but the main trends are properly reproduced.

We would like to comment at this point that reproduction of phonon dispersion curves has traditionally been considered a good check for accuracy of parameterized potentials. However, we have explicitly checked that good agreement with experimental or *ab initio* phonon dispersion curves at zero pressure does not guarantee that the potential will transfer properly to high pressure conditions. Our previously reported potentials,³⁻⁷ already quite complex in nature, generated almost perfect phonons at zero pressure⁷ and also very accurate pressure-volume relations and thermal expansivities,³ yet they do not produce correct high-pressure phonons. To our knowledge, this is the first time that a parameterized potential is reported that generates equally accurate phonons at any pressure.

To further test transferability to different bulk environments, we have calculated Schottky vacancy (SV) and stacking fault (SF) formation energies in MgO, and compared them to *ab initio* pseudopotential-GGA calculations performed by us using the SIESTA code.²⁴ The SV formation energy was estimated by removing one Mg^{2+} and one O^{2-} ion, chosen randomly from a 216 ion supercell. This means we have most probably not found the energetically most stable configuration, of experimental relevance, but for the purpose of direct comparison with the *ab initio* result on the same ionic configuration this is no problem. After removal, the positions of the remaining ions were relaxed. For the GAIM-relaxed configuration, forces calculated with SIESTA were smaller than $0.02 \text{ eV}/\text{\AA}$, showing that the relaxation pattern predicted by both codes is very similar. The Shottky formation energy calculated with the GAIM was $E_f(\text{Shottky})=8.1 \text{ eV}$, compared with 7.7 eV obtained with SIESTA.

As examples of planar extended defects, we generated two evenly spaced stacking faults, ten atomic layers apart, where the stacking sequence, along the (111) crystallographic direction, is changed from $a\beta c a b \gamma a \beta c a b \gamma \dots$ (where latin and greek letters denote anion and cation sublattices, respectively) to $a\beta c a b \gamma a \gamma b a c \beta a \gamma \dots$. After reoptimizing the lattice parameters, formation energies were evaluated. Our calculations give $E_f(\text{SF})=0.11 \text{ eV}$, while SIESTA predictions give 0.09 eV .

Next, we consider transferability to low-coordination environments. In Table I, we present formation energies and structural properties (relaxation and rumpling) of (100) and (110) rocksalt surface terminations, and compare them to representative *ab initio* DFT calculations.^{25,26} Both surfaces are modeled employing slabs [with 720 atoms, 20 atomic layers thick for (100) and 1120 atoms, 28 atomic layers thick for (110) termination] and three-dimensional periodic boundary conditions. A vacuum gap is created on both sides of the slab so that periodic replicas do not interact with each other. The slabs are cleaved from the geometry-optimized rocksalt structure, and the *lateral* dimensions are kept fixed during surface relaxation. All ions are allowed to relax, by a conjugate gradient method, until the force on each ion is smaller than $1 \text{ meV}/\text{\AA}$.

Relaxation and rumpling are defined as $\rho=(d_a+d_c-2d_b)/2d_b$ and $\epsilon=(d_a-d_c)/d_b$, respectively, where d_a , d_c are the interlayer distances for anions and cations at the surface, and d_b is the equilibrium interionic distance for bulk MgO.

TABLE I. Surface energies, in J/m^2 , and adimensional relaxation and rumpling for (100) and (110) MgO terminations, compared to *ab initio* DFT results (Refs. 25 and 26). In the last column, LDA(GGA) results are quoted. In the AIM column, the value in parenthesis gives the surface energy when the dispersion terms are enhanced for the anion in the surface layer, following Ref. 28.

| | AIM | Ref. 25 | Ref. 26 |
|-----------------|------------|---------|-------------|
| $E_f(100)$ | 1.20(1.05) | | 1.14(1.02) |
| $\rho(100)$ | -0.1 | -0.48 | -0.2(-0.2) |
| $\epsilon(100)$ | 1.5 | 1.62 | 1.8(2.2) |
| $E_f(110)$ | 2.60(2.32) | | 2.50(2.22) |
| $\rho(110)$ | -9.5 | | -8.9(-10.3) |
| $\epsilon(110)$ | 2.0 | | 1.7(1.7) |

The formation energy is defined as $E_f = (E_{\text{slab}} - NE_b) / 2A$, where E_{slab} is the total energy of the slab, E_b is the bulk lattice energy, N is the number of MgO units, and $2A$ is the total surface area of the slab.

Our results predict a small negative relaxation and small positive rumpling for the (100) termination, and larger structural modifications for the (110) termination, in line with the *ab initio* results. Also, the relative stability of both terminations is properly reproduced. [Alfonso *et al.*²⁷ give a more comprehensive comparison of experimental and theoretical results for the (100) termination.] It is interesting to note that our surface energies are closer to LDA results, even though the GAIM potential was fitted to GGA results. The (100) and (110) terminations contain oxide anions with coordination numbers equal to 5 and 4, respectively. These anions (see below) have higher polarizabilities than bulk anions and we consequently expect the surface ions to feel an enhanced dispersion attraction, which will stabilize the surface. The Slater-Kirkwood formula²⁸ may be used to predict the enhancement of the dispersion coefficients involving surface ions from their polarizabilities, which are predicted in the GAIM model. By using such enhanced dispersion coefficients for surface oxide anions, we obtain a surface energy in much better agreement with the GGA *ab initio* results (see Table I). We note, however, that GGA does not fully incorporate the highly nonlocal dispersion interactions, so this is just a tentative explanation.

It is also interesting to analyze the reasons for a positive rumpling, by modifying the potential by hand and observing the consequences. We have found that increasing or decreasing the oxide polarizabilities by 10% does not change the sign of rumpling. However, if we build a potential with just a 5% stronger oxide-oxide repulsion (the Mg-O overlap repulsion is correspondingly reduced so that the same equilibrium bulk distance results), the rumpling turns negative, indicating the high relevance of steric effects in determining MgO surface morphology, as suggested by Alfonso *et al.*²⁷ and Broqvist *et al.*²⁶

Finally, we have analyzed the GAIM performance on small $(\text{MgO})_n$ clusters. Figure 2 shows the coordination number dependence of the oxide polarizability for an unre-

laxed $(\text{MgO})_{64}$ cubic cluster (all distances equal to the bulk interionic distance), compared to coupled cluster results by Fowler and Tole.¹² Again, we notice that the internal consistency cycle in the GAIM is able to capture the polarizability increases in going from a bulk to a corner site. We stress here that the second term in Eq. (8) is crucial to achieve this level of agreement for clusters (while it is only of secondary importance to describe the polarizability variations in different bulk environments). Li *et al.* have studied the atomic relaxations in a cubic $(\text{MgO})_{64}$ cluster with *ab initio* LDA calculations.²⁹ Our relaxed interatomic distances agree with those given in Fig. 1 of Ref. 29 to better than 2% and, moreover, most of the discrepancy can be ascribed to the systematic differences between LDA and GGA calculations. This demonstrates that, by combining a force matching procedure with a physically based functional form for the potential, the “holy grail” of a fully transferable potential may indeed be realized.

IV. SUMMARY

A generalization of our previously reported aspherical ion model (AIM) potential for MgO has been described. The motivation for the realization of this GAIM potential was the ambitious goal of generating a fully transferable potential model, which would be highly beneficial for the large-scale computer simulation of complex physical phenomena in materials science and geoscience. The GAIM potential incorporates a functional description of the charge density of the oxide anion (mean radius of the anion, dipolar and quadrupolar induction and shape distortions), and of its response to changes in the atomic environment. Moreover, the susceptibilities governing the induction of multipoles and shape distortions are themselves dependent on the atomic environment in the GAIM potential, which allows a reproduction of the pressure and coordination number dependencies of oxide polarizabilities, for example. The GAIM potential has been tested by performing benchmark calculations of structural and dynamical properties in several representative atomic coordination environments. This way, we have shown our potential to describe accurately atomic interactions for both the bulk (for arbitrary pressure and temperature conditions within the range of geophysical relevance), point and extended bulk imperfections, different surface terminations and small clusters. In a separate publication,³⁰ we show that the GAIM also gives a realistic description of the MgO melting curve, a problem of current geophysical interest. The potential thus also transfers properly to the liquid phase.

To finish this article, we stress that by “full transferability” we mean that we expect to obtain an accurate description of atomic interactions for all those situations not involving electron itineracy. For example, partial metalization is a possible stabilization mechanism for polar surface terminations such as MgO(111). Our potential is not expected to provide good results in these problematic cases. Also, there have been previous attempts to generate variable-charge potentials which transfer between different charge states (which are useful for simulation of complex oxides such as TiO_2), but Thomas *et al.*¹¹ have shown that the electrostatic part of

these potentials is not realistic, as the predicted ionic charges are systematically too low.⁹ Our potential model, without a proper generalization, is not expected to work in these cases either. Nevertheless, there are lots of interesting problems in materials science and geophysics that can be addressed with our transferable ionic potential.

ACKNOWLEDGMENTS

This work was supported by Junta de Castilla y León (Project No. VA073/02) and DGES (Project No. MAT2002-04393-C02-01). A. A. also acknowledges financial support under the “Ramón y Cajal” program.

*Electronic address: aguado@metodos.fam.cie.uva.es

- ¹A. Laio, S. Bernard, G. L. Chiarotti, S. Scandolo, and E. Tosatti, *Science* **287**, 102 (2000).
- ²A. J. Stone, *Theory of Intermolecular Forces* (Oxford University Press, Oxford 1996).
- ³A. Aguado, L. Bernasconi, and P. A. Madden, *Chem. Phys. Lett.* **356**, 437 (2002).
- ⁴A. Aguado, L. Bernasconi, and P. A. Madden, *J. Chem. Phys.* **118**, 5704 (2003).
- ⁵A. Aguado and P. A. Madden, *J. Chem. Phys.* **118**, 5718 (2003).
- ⁶A. Aguado, L. Bernasconi, S. Jahn, and P. A. Madden, *Faraday Discuss.* **124**, 171 (2003).
- ⁷A. Aguado and P. A. Madden, *J. Chem. Phys.* **119**, 7471 (2003).
- ⁸P. Tangney and S. Scandolo, *J. Chem. Phys.* **119**, 9673 (2003).
- ⁹V. Swamy and J. D. Gale, *Phys. Rev. B* **62**, 5406 (2000).
- ¹⁰F. Calvo, *Phys. Rev. B* **67**, 161403 (R) (2003).
- ¹¹B. S. Thomas, N. A. Marks, and B. D. Begg, *Phys. Rev. B* **69**, 144122 (2004).
- ¹²P. W. Fowler and P. Tole, *Surf. Sci.* **197**, 457 (1988).
- ¹³N. C. Pyper, *Mol. Phys.* **95**, 1 (1998).
- ¹⁴A. Aguado and J. M. López, *J. Phys. Chem. B* **104**, 8398 (2000).
- ¹⁵K. T. Tang and J. P. Toennies, *J. Chem. Phys.* **80**, 3726 (1984).
- ¹⁶M. Wilson, P. A. Madden, and B. J. Costa Cabral, *J. Phys. Chem.* **100**, 1227 (1996).
- ¹⁷A. Aguado, M. Wilson, and P. A. Madden, *J. Chem. Phys.* **115**,

- ¹⁸P. Jemmer, P. W. Fowler, M. Wilson, and P. A. Madden, *J. Phys. Chem. A* **102**, 8377 (1998).
- ¹⁹A. J. Rowley, M. Wilson, and P. A. Madden *J. Phys.: Condens. Matter* **11**, 1903 (1999).
- ²⁰M. C. Payne, M. P. Teter, D. C. Allan, T. A. Arias, and J. D. Joannopoulos, *Rev. Mod. Phys.* **64**, 1045 (1992).
- ²¹J. P. Perdew, *Physica B* **172**, 1 (1991).
- ²²A. R. Oganov, M. J. Gillan, and G. D. Price, *J. Chem. Phys.* **118**, 10174 (2003).
- ²³S. Baroni, S. de Gironcoli, A. Dal Corso, and P. Giannozzi, *Rev. Mod. Phys.* **73**, 515 (2001).
- ²⁴J. M. Soler, E. Artacho, J. D. Gale, A. García, J. Junquera, P. Ordejón, and D. Sánchez-Portal, *J. Phys.: Condens. Matter* **14**, 2745 (2002).
- ²⁵Y. Yan, M. F. Crisholm, S. J. Pennycook, and S. T. Pantelides, *Surf. Sci.* **442**, 251 (1999).
- ²⁶P. Broqvist, H. Grönbeck, and I. Panas, *Surf. Sci.* **554**, 262 (2004).
- ²⁷D. R. Alfonso, J. A. Snyder, J. E. Jaffe, A. C. Hess, and M. Gutowski, *Phys. Rev. B* **62**, 8318 (2000).
- ²⁸J. C. Slater and J. G. Kirkwood, *Phys. Rev.* **37**, 682 (1931).
- ²⁹Y. Li, D. C. Langreth, and M. R. Pederson, *Phys. Rev. B* **55**, 16456 (1997).
- ³⁰A. Aguado and P. A. Madden, unpublished results.